

Frequency Optimization of Lunar Rover Wireless Power Transfer System with Multi-layer Insulation

Mingyang CHEN¹, Bingcheng JI¹, Katsuhiro HATA², Takehiro IMURA³, Hiroshi FUJIMOTO¹
Yoichi HORI¹, Shuhei SHIMADA⁴, Sayuri HONDA⁴, Osamu KAWASAKI⁴

¹ Department of Advanced Energy, Graduate School of Frontier Sciences, University of Tokyo
chin.meiyu19@ae.k.u-tokyo.ac.jp

² Department of Informatics and Electronics, Institute of Industrial Science, University of Tokyo

³ Department of Electrical Engineering, Tokyo University of Science

⁴ Reseach Unit I, R&D Directorate, Japan Aerospace Exploration Agency

Abstract In the lunar rover wireless power transfer system, the heat leakage caused by the wire connection between the solar panel and rover body can be avoided. However, in order to achieve thermal insulation of the rover body, the metal MLI materials should be placed between the WPT coils indicating the power transfer property will be influenced. In this paper, the WPT system with the MLI materials power transfer property enhancement with frequency variation is investigated, and an equivalent electric regression model is proposed to explain the MLI materials influence to the WPT system. Then the optimal frequency for maximum efficiency is calculated.

Key words Lunar rover, wireless power transfer, multi-layer insulation, frequency optimization, frequency-dependent resistance

1 Introduction

Recently the wireless power transfer(WPT) [1] based on magnetic resonance has been applied in various areas. Operating at the resonance frequency, WPT has become a promising solution to replace the wires with a high transfer efficiency. Because of this property, WPT can be applied in the space exploration field, such as the lunar rovers.

Lunar rover is an electric vehicle used for conducting research tasks on the lunar surface. Because of the intense temperature variation between the lunar day and night, the heat leakage needs to be avoided to protect the devices in the lunar rover. In order to achieve thermal isolation, Multi-layer Insulation(MLI) materials [2], made of aluminum layers of 200-300 nm, are used for covering the lunar rover body. MLI materials, as shown in Fig. 1(a)(b), are metal thermal isolation materials, which are employed in the space exploration area.

However, there are also parts that cannot be covered with MLI materials. The conventional lunar rover is usually powered by photovoltaic(PV) panels, which are connected to the rover's body by wires not covered by MLI. The heat dissipated from the PV panels and wires can not be ignored [3].

To solve this problem, systems using wireless power transfer to replace the wires between the PV panel and the lunar rover have been proposed recently [4], which can avoid the heat leakage from the wire. In the system, the MLI materials are placed between the transmitter the receiver coils, because the receiver coil is placed inside the rover's body. MLI is made of aluminum, so it can be seen as layers of metal placed between two

coils. Due to the isolation effect of metal conductor material on magnetic field, the efficiency of WPT system decreases at the same resonance frequency. Searching for the optimal frequency is one of the ways to compensate for this loss of efficiency.

For the WPT systems on earth, in order to avoid the interference of radio waves, there are regulations for WPT frequencies. However, for lunar rover WPT systems, a large range of frequency can be employed as operating frequency. Previous researches for frequency optimization in the air usually focus on the copper loss of coils. Based on the Ohmic resistance analysis, the quality factor optimization under frequency variation is conducted [6] [7] [8] to search the optimal resonance frequency. In ref [9], powerelectronics losses have also been taken into consideration to conduct a numerical model for the optimal resonance frequency.

However, none of these researches considered the case of metal materials between two coils. The frequency optimization in underwater WPT systems for autonomous underwater vehicles [10] [11] is similar to this case. Because the power loss caused by sea water between the transmitter and receiver coil is generated by the eddy current inside the seawater, which is similar to a metal materials. In references [10]- [14] the eddy current loss in the seawater have been analysed. The most precise calculation for occasions with ferrite and without ferrite are proposed in the ref [10] and [11], respectively. But there are certain difference between water and metal materials. Furthermore the recent researches for underwater WPT frequency optimization haven't considered the copper loss of the coils.

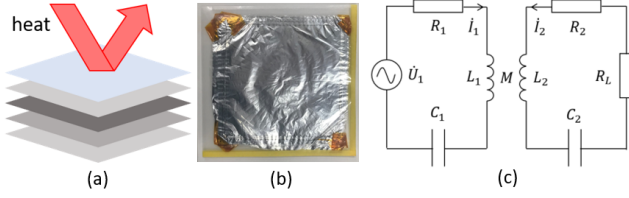


Figure 1: (a) Profile of MLI structure. (b) JAXA MLI. (c) Employed SS topology.

Taking the MLI materials into consideration, this paper investigated the WPT system property of a Qi [5] coil WPT system with frequency variation. Analysis has been carried out to explain the frequency-dependent influence of the system, and an electrical model based on the theoretical analysis as well as ordinary linear squared(OLS) regression has been established to calculate the optimal frequency of WPT systems with MLI materials. In further studies, the analysis method and regression model can be used to conduct the closed-form formulas of optimal resonance frequency for general WPT systems with metal materials placed between different coils. The MLI materials applied in this paper are special designed by JAXA, with slits in radioactive shape. This design reduces the blockage of the magnetic field by MLI.

This paper is organized as follows, section 2 analyzes the frequency-dependent parameters of the WPT maximum efficiency function. In section 3, a regression model considering the influence of the copper losses and the eddy current loss in the MLI materials is established. In section 4, coils are measured to discuss the influence of MLI material towards the frequency dependent property of the coils. In section 5, the regression analysis based on the proposed model is conducted, and the optimal frequency is calculated and discussed. In section 6, the conclusion is summarized.

2 WPT Efficiency Analysis

In this paper, the SS topology has been employed as shown in Fig. 1(c). And the resonance frequency of maximum efficiency is considered as the optimal resonance frequency. For WPT systems, the circuit equations are shown as follows.

$$\begin{cases} \left(R_1 + j\omega L_1 + \frac{1}{j\omega C_1} \right) \cdot \dot{I}_1 + j\omega M \cdot \dot{I}_2 = \dot{U}_s \\ j\omega M \cdot \dot{I}_1 + \left(R_2 + R_L + j\omega L_2 + \frac{1}{j\omega C_2} \right) \cdot \dot{I}_2 = 0 \end{cases} \quad (1)$$

Where R_1 and R_2 are the resistance of the first side and secondary side; L_1 , L_2 and C_1 , C_2 are the self-inductances and capacitance of the first and secondary side, respectively; \dot{U}_s is the input power; \dot{I}_1 and \dot{I}_2 is the first and secondary side current, respectively. ω is the angle frequency and M is the mutual inductance of two coils. R_L is the load resistance. at the resonance frequency, the inductance and capacitance of both sides

cancel with each other:

$$\omega L_1 = \frac{1}{j\omega C_1}, \omega L_2 = \frac{1}{j\omega C_2} \quad (2)$$

Then the efficiency of the system can be calculated as:

$$\eta = \frac{\omega^2 M^2 R_L}{(R_2 + R_L)(R_1 R_2 + R_1 R_L + \omega^2 M^2)} \quad (3)$$

Based on this equation, derivate the η by R_L when

$$R_L = R_{L-\eta max} = \sqrt{R_2 \left(\frac{\omega^2 M^2}{R_1} + R_2 \right)} \quad (4)$$

The efficiency achieves the maximum point at this resonance frequency [4]:

$$\eta_{max} = \frac{\omega^2 M^2 R_{L-\eta max}}{(R_2 + R_{L-\eta max})(R_1 R_2 + R_1 R_{L-\eta max} + \omega^2 M^2)} \quad (5)$$

From these equations, it is observed that the efficiency is a multivariate function of ω , M , R_1 and R_2 . Based on this, we can set maximum efficiency objective function:

$$\eta = \eta(R_1, R_2, M, \omega) \quad (6)$$

In this paper, we only consider the change in frequency, so we can consider ω , R_1 , R_2 , M as the intermediate variables. The frequency is the only independent variable, and then the function can be obtained:

$$\eta = \eta(R_1(f), R_2(f), M(f), \omega(f)) \quad (7)$$

In order to get a numerical equation of the efficiency function, it is necessary to establish equations for the resistance and mutual inductance.

3 WPT Coil Resistance Regression Model Establishment

According to measurement data and previous researches, compared to the resistance, mutual inductance can be seen as a constant, which can be easily measured at an arbitrary frequency. The rest of three intermediate variable mentioned in section 2 are $R_1(f)$, $R_2(f)$, $\omega(f)$. $\omega(f)$ equals to $2\pi f$, so as long as $R(f)$ is determined, the relation between the maximum efficiency and resonance frequency can be derived. Previous researchers have done plenty of numerical models for frequency-dependent resistance of litz-wire coils. The frequency-dependent resistance of litz-wire coils consist of two parts: the conductivity resistance caused by net current and the proximity resistance caused by the eddy current inside the wires.

$$R(f) = R_{cond} + R_{pr} \quad (8)$$

For conductivity losses, according to previous researches, it can be concluded that when the radius of

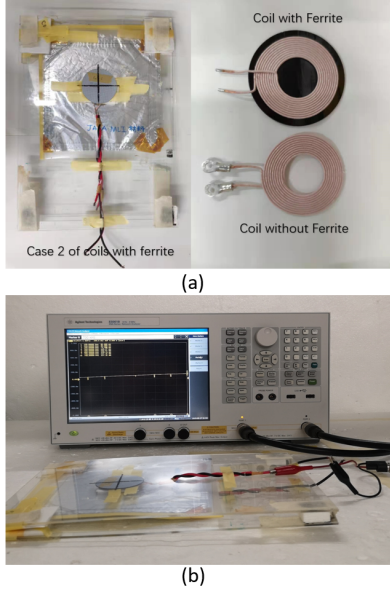


Figure 2: (a) Employed coil structure (b) Experiment platform

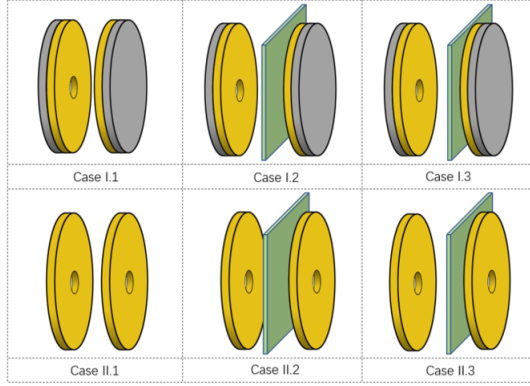


Figure 3: Measurement Cases

each strand r_s in litz wire is relatively small compared to the skin depth δ , the skin effect can be ignored:

$$F_R = \frac{R_{cond}}{R_{dc}} \approx 1 + \frac{1}{48} \left(\frac{r_s}{\delta} \right)^4 \approx 1 \quad (9)$$

where:

$$\delta = \frac{\sqrt{2}}{\sqrt{\mu\sigma\omega}} \quad (10)$$

Where μ is the permeability and the σ is the conductivity of the material. n_0 is the number of the strands in a single litz wire. R_{cond} is the conductivity resistance of a unit length wire. It can be observed that for general litz-wire coils, the radius of each strand is small (For example the coils employed), the conductivity resistance is a constant when the coil is fixed.

For proximity effect, the eddy current loss per unit length inside an arbitrary coil caused by the alternating magnetic field will be proportional to frequency squared [7].

$$P_j = \frac{\pi\gamma^4 H_j^2}{8\sigma} \quad (11)$$

where

$$\gamma = \sqrt{2}r_s/\delta = r_s\sqrt{\mu\sigma\omega} \quad (12)$$

under the circumstance of $\gamma < 1$. P_j and H_j represent the power loss per unit length caused by proximity effect and H-field intensity of the j_{th} turn. Because the H-field intensity for j_{th} turn is proportional to the net current and the equivalent proximity resistance for a strand of unit length in the j_{th} turn is:

$$\begin{aligned} R_j &= \frac{P_j}{(I_{rms}/n_0)^2} = \frac{2P_j}{(I/n_0)^2} \\ &= \frac{2n_0^2 P_j}{I^2} \end{aligned} \quad (13)$$

It can be inferred from (11) and (12) that the ratio of H_j^2 to I^2 will be independent of frequency. The resistance caused by the proximity effect will be proportional to frequency squared. Thus the frequency-dependent regression model for litz wire coils is:

$$R(f) = R_{cond} + R_{pr} = k_{cond} + k_{pr}f^2 \quad (14)$$

Where k_{cond} is a constant, equals to the DC resistance. k_{pr} is another constant related to the magnetic field distribution of the coil. The calculation of the factors is out of scope for this paper, detailed models are in ref [7] [8].

But these conventional formulas cannot explain the increase of resistance caused by the MLI materials. So in this section, a novel electric regression model has been proposed by adding an equivalent resistance representing the MLI influence into the resistance model.

Because the power loss of eddy current for a certain conductor between transmitter and receiver coils can be obtained as follows [10] [15].

$$P_{eddy} = k_{eddy1}I_1^2f^2 + k_{eddy2}I_2^2f^2 \quad (15)$$

Where k_{eddy1} and k_{eddy2} are the complex multiple integrals representing the position and structure where eddy current exists [10]. Thus the value of k_{eddy1} and k_{eddy2} are constant under frequency variation. I_1 and I_2 are the coil RMS currents of the transmitter and receiver side generating the electric field inside the integral domain. f is the frequency of the magnetic field, which equals to the frequency of the alternating current. It is assumed that the external eddy current caused by the coil increases the equivalent resistance of each coil, so the eddy current loss is added to the coil copper loss to establish an equivalent resistance model. So the final resistance model for transmitter and receiver coils is:

$$\begin{aligned} R(f) &= \frac{P_{cond} + P_{prox} + P_{eddy}}{I^2} \\ &= k_{cond} + k_{pr}f^2 + k_{eddy}f^2 = k_{cond} + k_{total}f^2 \end{aligned} \quad (16)$$

To verify this regression model and to analyze the influence of the MLI materials towards the optimal frequency, in section 4, the properties for a pair of coils are measured and discussed.

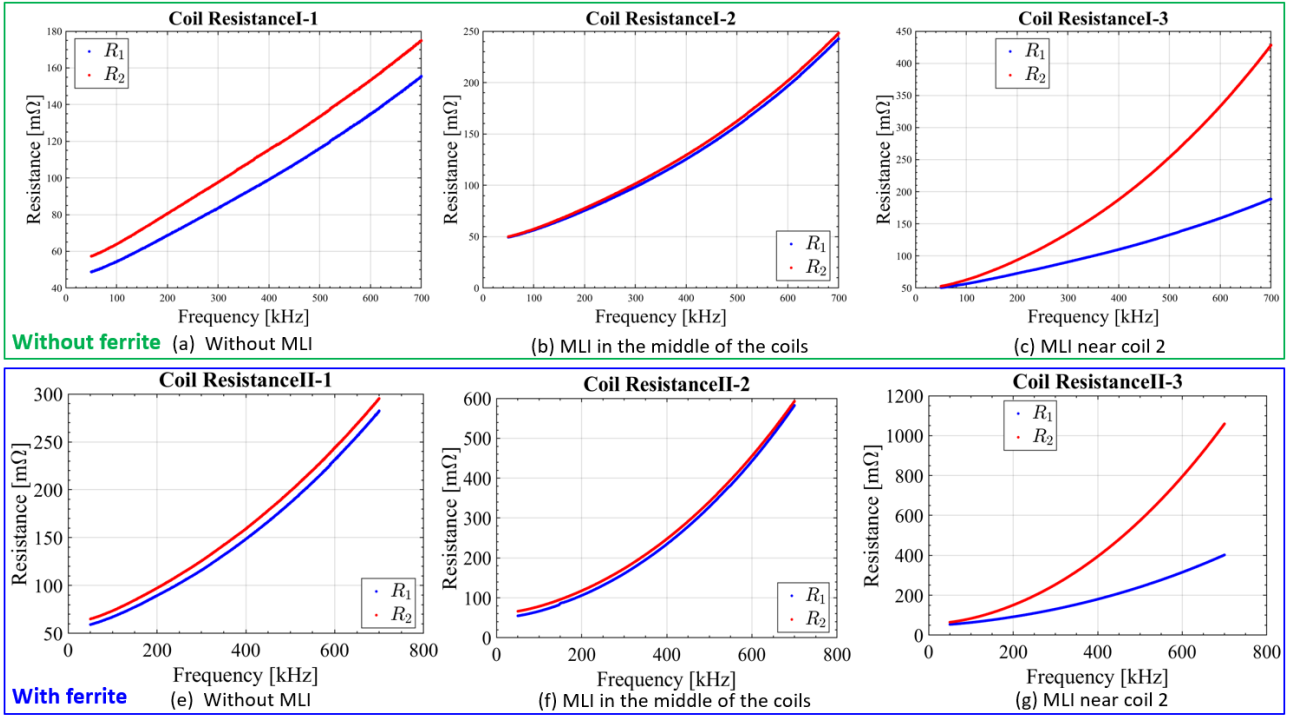


Figure 4: Resistance of the coils with and without ferrite in case I-II

4 Coil Parameter Measurement Experiment

The employed coils are shown in Fig. 2(a), the experiment platform is in Fig. 2(b). The distance between two coils is 10 mm, and three cases for two types of coils have been measured as shown in Fig. 3. The first case is without MLI materials. In the second case, MLI materials is placed in the middle of two coils. In the third case, MLI materials is placed near (about 1mm) the secondary coil. The difference of two types of coils is whether the ferrite exists. The coils are TDK 10K2-A11-6-T170909 based on A11 specification of Qi [5], using AWG17 type 2 litz wire consists of 105 AWG40 strands. Measurement is carried out using KEYSIGHT E4990A Impedance Analyzer and the Agilent Technologies E5061B Network Analyzer, with both devices resulting in similar data. Frequency range is chosen to be 50-700kHz, because higher frequency leads to increasing hardware costs, while below 50kHz the quality factor is usually insufficient. The resistance of the coils with or without ferrite is shown in Fig. 4. It can be observed in Fig. 4 that the resistance increases with the frequency in all cases, and the MLI materials adds to the measured resistance of the coils in Fig. 4(c) and Fig. 4(g). The closer the MLI materials is, the higher the coil resistance increases. This is because the eddy current loss in MLI materials depends on the magnetic field, and the magnetic field strength is stronger near the coils. Comparing with the coils without ferrite, the coils with ferrite possess a higher resistance because of a higher magnetic strength. This is because the H field

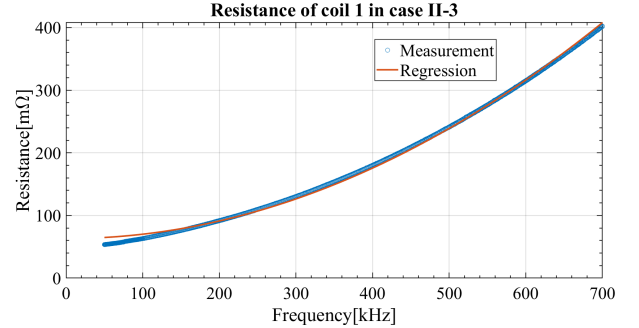


Figure 5: Regression and measurement data for coil 1 in case II-3

influences the skin and proximity effects of the coil, and the eddy current in the MLI materials. Another property taken into consideration is the mutual inductance. Compared with the resistance, the frequency-dependent variation of mutual inductance is not significant. But the influence of MLI materials is obvious, due to the block of magnetic field, and MLI reduces the mutual inductance. In the rough calculation of optimal frequency, mutual inductances can be considered as a constant.

5 WPT Frequency Optimization

Based on the regression model, the OLS regression has been conducted. The objective is to verify the analysis and to estimate the factors and to calculate the optimized frequency for the coils. The regression result is shown in tables and curves below. The estimation of

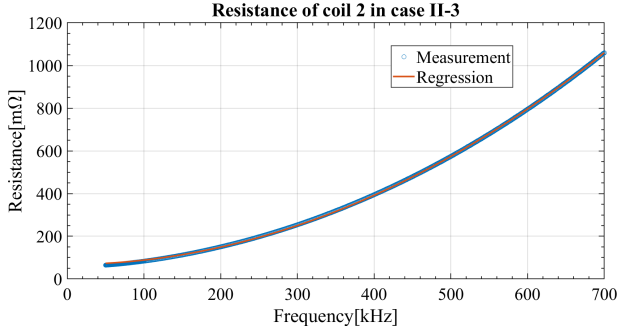


Figure 6: Regression and measurement data for for coil 2 in case II-3

Table 1: Estimated result of k_{cond}

cases	1	2	3
Coil 1 I	0.06028	0.05958	0.06154
Coil 2 I	0.07150	0.06143	0.06257
Coil 1 II	0.07125	0.06168	0.06308
Coil 2 II	0.07889	0.07398	0.06825

Table 2: Estimated result of k_{total}

cases	1	2	3
Coil 1 I	2.103e-13	3.848e-13	2.737e-13
Coil 2 I	2.315e-13	3.939e-13	7.559e-13
Coil 1 II	4.474e-13	1.063e-12	7.034e-13
Coil 2 II	4.618e-13	1.063e-12	2.023e-12

parameter k_{cond} and k_{total} is shown in Tab. 1 and 2.

Both k_{cond} and k_{total} have a high confidence level of T-statistics ($> 99.99\%$), and R^2 of the regressions is always higher than 96%. From the estimation parameters, it can be concluded that k_{cond} is similar to each other, representing the fixed conducting resistance, and the difference is because of the different length of connecting wires during the measurement and measurement errors. For k_{total} , it can be observed that the MLI materials' influence on resistance has the same order of magnitude as the proximity effect. This may be because of both losses are proportional to H-field squared.

The comparison between the regression resistance and measurement is shown in Fig. 5-6. Due to the space limitation, other regression curves are not included in the paper.

It can be observed for the regression model, to a large extent, the variation of resistance is explained. The higher the resistance is, the better the data fits the model. Based on these regression results, the numerical solutions for optimal frequency are calculated. The M at 50 kHz is chosen to calculate the relation of maximum efficiency and resonance frequency. The calculation result is shown in Fig. 7(a),(b). The optimized frequency calculated by the regression models is: 545.4kHz for case I-1; 394.2kHz for case I-2; 369.4kHz for for case I-3. For the systems with ferrite, in the three

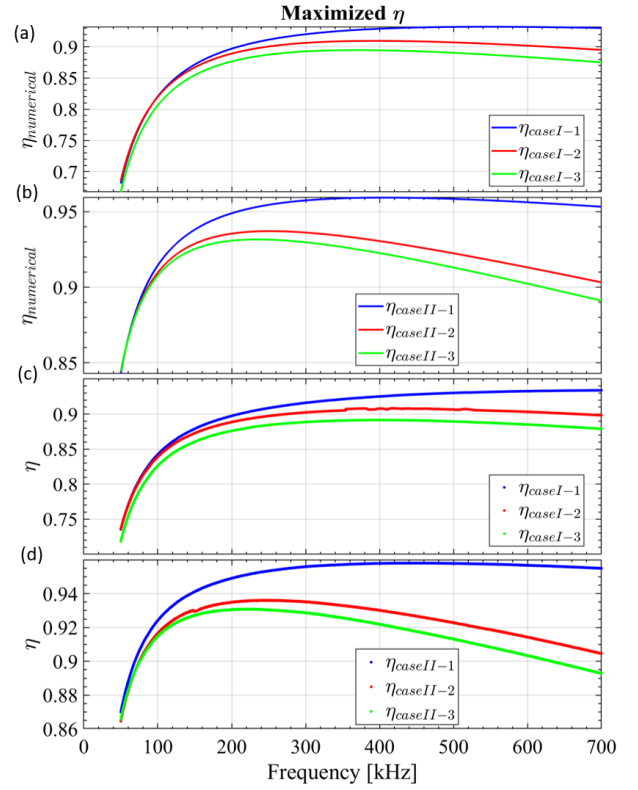


Figure 7: (a) Numerical estimation of maximum efficiency for case I. (b) Numerical estimation of maximum efficiency for case II. (c) Measured maximum efficiency for case I. (d) Measured maximum efficiency for case II.

cases, the optimized frequencies are 406.1kHz, 252.0kHz and 234.5kHz, respectively. MLI and the ferrite reduces the optimal resonance frequency. Ferrite can improve the maximum efficiency at lower frequencies, but when there are MLI materials, the efficiency drops more rapidly with respect to the frequency in a higher frequency range.

Compared with efficiency at 85kHz, the efficiency at optimal frequency increases largely, for case I at 85kHz, η is 82.25%, 82.03% and 80.63% respectively. But the efficiency at the optimal frequencies is 93.39%, 90.84% and 89.17%. For case II, at 85kHz, the efficiency is 91.47%, 90.78%, 90.67%, respectively. The corresponding maximum efficiency at optimal frequencies is 95.81%, 93.62% and 93.1%, respectively.

The case when MLI nears one coil possesses the lowest maximum efficiency and optimal frequency, although in this case the transmitter coil has a lower resistance than the case of MLI material in the middle of two coils. This may be because the symmetric structure has a higher efficiency, and the increase of the resistance of the secondary coil (R_2) is larger than the decrease of R_1 . The efficiency curves based on calculating the measured data directly by (5) have been shown in Fig. 7(c)(d). It can be observed that the regression model agrees with the measurement. For arbitrary WPT systems with MLI, the regression model can be applied to establish a numerical model of frequency-dependent maximum effi-

ciency with few data. The limitation of this work is that the regression model is not a closed-form solution for frequency optimization, which needs measurement data to establish a numerical formula when applying to other coils.

Because the measurement data is not always available, further researches are needed to establish a specific model. Based on the conclusion of this paper, by developing the functions of the factors in the proposed regression model, further studies can propose more specific formulas to explain the maximum efficiency at different frequencies.

6 Conclusion

In this paper, the optimal frequency of WPT systems with MLI material for lunar rovers has been analyzed. The circuit analysis shows the maximum efficiency depends on the resistance and mutual inductance. Then an equivalent resistance regression model taking the eddy current loss inside the MLI material into consideration has been proposed. Based on the measurement using a specialized structure, the sensitivity of resistance and mutual inductance towards the resonance frequency have been discussed. The regression analysis for WPT systems shows the model agrees with the measurement result. Based on the regression result, specialized numerical formulas of the maximum efficiency have been calculated, based on the results, the influence of MLI and ferrite in such WPT system has been discussed. Both the ferrite and MLI tend to reduce the system optimal frequency, although their influence on the maximum efficiency is contrary with each other.

7 Acknowledgment

This work was partly supported by JSPS KAKENHI Grant Number 19H02123.

References

- [1] Imura, Takehiro, and Yoichi Hori. "Maximizing air gap and efficiency of magnetic resonance coupling for wireless power transfer using equivalent circuit and Neumann formula." *IEEE Transactions on industrial electronics* 58.10 (2011): 4746-4752.
- [2] BJingshan J. Multilayer Insulation Materials and Their Application to Spacecrafts[J]. *AEROSPACE MATERIALS & TECHNOLOGY*, 2000, 4.
- [3] Hickman J M, Curtis H B, Landis G A. Design consideration for lunar based photovoltaic power systems[C]//*IEEE Conference on Photovoltaic Specialists*. IEEE, 1990: 1256-1262.
- [4] Ji B, Hata K, Imura T, et al. Basic Study of Solar Battery Powered Wireless Power Transfer System with MPPT Mode and DC Bus Stabilization for Lunar Rover[C]//*IECON 2018-44th Annual Conference of the IEEE Industrial Electronics Society*. IEEE, 2018: 4787-4792.
- [5] Wireless Power Consortium. The Qi wireless power transfer system power class 0 specification[J]. 2017.
- [6] Kim J, Park Y J. Approximate closed-form formula for calculating ohmic resistance in coils of parallel round wires with unequal pitches[J]. *IEEE transactions on Industrial Electronics*, 2014, 62(6): 3482-3489.
- [7] Deng Q, Liu J, Czarkowski D, et al. Frequency-dependent resistance of litz-wire square solenoid coils and quality factor optimization for wireless power transfer[J]. *IEEE Transactions on Industrial Electronics*, 2016, 63(5): 2825-2837.
- [8] Acero J, Alonso R, Burdío J M, et al. Frequency-dependent resistance in Litz-wire planar windings for domestic induction heating appliances[J]. *IEEE Transactions on Power Electronics*, 2006, 21(4): 856-866.
- [9] Zhou H, Gao X, Lai J, et al. Natural frequency optimization of wireless power systems on power transmission lines[J]. *IEEE Access*, 2018, 6: 14038-14047.
- [10] Yan Z, Zhang Y, Kan T, et al. Frequency optimization of a loosely coupled underwater wireless power transfer system considering eddy current loss[J]. *IEEE Transactions on Industrial Electronics*, 2018, 66(5): 3468-3476.
- [11] Zhou J, Li D, Chen Y. Frequency selection of an inductive contactless power transmission system for ocean observing[J]. *Ocean Engineering*, 2013, 60: 175-185.
- [12] Itoh R, Sawahara Y, Ishizaki T, et al. Wireless power transfer to moving ornamental robot fish in aquarium[C]//*2014 IEEE 3rd Global Conference on Consumer Electronics (GCCE)*. IEEE, 2014: 459-460.
- [13] Yan Z, Zhang K, Wen H, et al. Research on characteristics of contactless power transmission device for autonomous underwater vehicle[C]//*OCEANS 2016-Shanghai*. IEEE, 2016: 1-5.
- [14] Zhou J, Li D, Chen Y. Frequency selection of an inductive contactless power transmission system for ocean observing[J]. *Ocean Engineering*, 2013, 60: 175-185.
- [15] F. Fiorillo, *Measurement and characterization of magnetic materials*, Elsevier Academic Press, 2004, ISBN 0-12-257251-3, page. 31